

UDC 541.6:548.737

A DFT STUDY ON THE GEOMETRY, SPECTROSCOPIC PROPERTIES,  
AND TAUTOMERIZATION OF THE LOCAL ANAESTHETIC DRUG PRILOCAINE

F. Heshmatipour<sup>1</sup>, S.A. Beyramabadi<sup>1,2</sup>, A. Morsali<sup>1,2</sup>, M.M. Heravi<sup>1</sup>

<sup>1</sup>Department of Chemistry, Mashhad Branch, Islamic Azad University, Mashhad, Iran

E-mail: beyramabadi@yahoo.com

<sup>2</sup>Research Center for Animal Development Applied Biology, Mashhad Branch, Islamic Azad University, Mashhad, Iran

Received May, 26, 2015

The prilocaine is a significant amino amide local anaesthetic. This drug can exist as three possible tautomers. Herein, by using density functional theory (DFT), and handling the solvent effects with the PCM model, the structure, energetic behavior, kinetics and mechanism of tautomerization, as well as the natural bond orbital analysis (NBO) of the prilocaine are reported. **P1** is the most stable tautomer of the prilocaine, which can be tautomerized to two other tautomers *via* the intramolecular-proton transfer. Good agreement between the calculated NMR chemical shifts and IR vibrational frequencies with the experimental values approves the suitability of the optimized geometry for the prilocaine. A large HOMO—LUMO energy gap implies a high stability of the prilocaine.

DOI: 10.15372/JSC20160606

**Key words:** prilocaine, DFT, tautomerization, intramolecular proton transfer, PCM.

## INTRODUCTION

Prilocaine or (RS)-N-(2-methylphenyl)-N<sup>2</sup>-propylalaninamide is an amino amide local anaesthetic. Its clinical profile is similar to that of the lidocaine. However, the prilocaine is metabolized more rapidly, and consequently, has lower toxicity than the lidocaine [ 1—4 ]. This important advantage means that the prilocaine is often considered as the safest choice for intravenous regional anaesthesia [ 5, 6 ].

The prilocaine has longer anaesthetic effects than the other amide anaesthetics [ 7 ]. It is used in dentistry, and in combination with the lidocaine is used in treatment of paresthesia-like conditions. Because of low cardiac toxicity, it is commonly used for intravenous regional anaesthesia, too [ 8 ]. In its injectable form, the trade name of the prilocaine drug is citanest. Claes Tegner and Nils Lofgren were the first to report the synthesis of the prilocaine [ 9 ].

Nowadays, the DFT methods are widely employed in many areas of the computational chemistry, such as investigations of the reaction kinetics and mechanisms, spectroscopic assignments, the characterization of molecular structures, drug science, and so on [ 10—13 ].

Previously, some aspect of the prilocaine properties has been investigated theoretically [ 14 ]. The knowledge of the structural and spectroscopic properties of drugs is an essential prerequisite for understanding their biological activity. Since, an accurate and detailed computational investigation on the prilocaine is of major importance. Herein, we address this issue and examine its molecular geometry, tautomerism, vibrational frequencies, NMR chemical shifts and the natural bond orbital (NBO) analysis using DFT approaches.

## COMPUTATIONAL METHODS

In this work, all of the calculations have been performed using the Gaussian 03 software package [15], where the B3LYP [16] functional and the 6-311+G(*d,p*) basis set were used. For the investigation of solvent effects in an aqueous solution, one of the self-consistent reaction field methods, the sophisticated polarized continuum model (PCM) [17] has been employed.

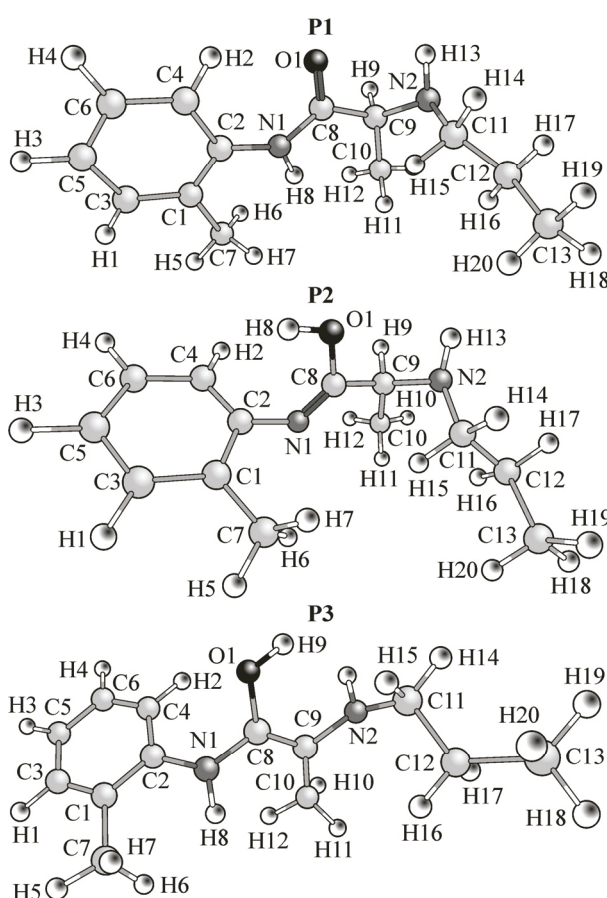
First, all geometries were fully optimized. The optimized geometries were confirmed to have no imaginary frequencies, except for transition states (TSs), which have only one imaginary frequency of the Hessian. The zero-point corrections and thermal corrections have been considered in the energy evaluation. The optimized geometry was used to compute the vibrational frequencies, NMR chemical shifts, atomic charges, and NBO analysis.

Since the DFT calculated vibrational frequencies are usually higher than the experimental ones, they were scaled using a factor of 0.9614 [18]. The <sup>1</sup>H shielding constants ( $\sigma$ ) of the prilocaine and of the reference TMS were computed by the gauge independent atomic orbital (GIAO) method [19] at the B3LYP/6-311+G(*d,p*) level. All structures were visualized using the Chemcraft 1.7 program [20].

## RESULTS AND DISCUSSION

**Molecular geometry.** The prilocaine can exist as three possible tautomers whose geometries have been fully optimized in the gas phase and an aqueous solution in PCM model. The PCM optimized geometries are shown in Fig. 1.

As seen in Fig. 1, in the **P2** tautomer the H8 proton transfers from the N1 atom to the O1 atom *via* an intramolecular proton transfer (IPT), in comparison with **P1**. Similarly, in the **P3** tautomer the H9 proton transfers from the C9 atom to the O1 atom, with respect to **P1**. Important structural parameters of the optimized geometries are listed in Table 2, where the zero-point corrections have been considered. As seen, **P1** is the most stable tautomer of the prilocaine in both gas phase and aqueous solution.



**Mechanism of tautomerization.** **P1** is the most stable tautomer of the prilocaine, which can be converted to **P2** and finally to **P3** *via* IPT. Herein, tautomerism of the prilocaine has been investigated using valuable DFT methods, which are used in the theoretical investigation of chemical reactions [10–13].

The TS of the **P1**↔**P2** tautomerization was named as **TSP1—P2**. The optimized geometry of **TSP1—P2** is shown in Fig. 2, in which the cleavage of the N1—H8 bond together with the formation of the O1—H8 bond is clear. In the **TSP1—P2** structure, the O1—H8 and N1—H8 bond lengths are 1.29 and 1.34 Å respectively. These bond lengths are 3.14 and 1.00 Å, for the **P1** tautomer, respectively, which are 0.96 and 2.43 Å in the optimized geometry of the **P2** tautomer, respectively.

**TSP1—P3** is TS of the **P1**↔**P3** tautomerization, the optimized geometry of which is shown in Fig. 2. In this structure, the cleavage of the

Fig. 1. Optimized geometries for **P1—P3** tautomers of the prilocaine

C9—H9 bond together with the formation of the O1—H9 bond is clear. In the **P1** tautomer, the C9—H9 and O1—H9 bond lengths are 1.09 and 2.76 Å, respectively, which change to 1.58 and 1.20 Å, respectively, in the optimized geometry of **TSP1—P3**. In the optimized geometry of the **P3** tautomer, these bond lengths are 2.45 and 0.96 Å, respectively.

TS of the **P2**↔**P3** tautomerization was named as **TSP2—P3**. The optimized geometry of **TSP2—P3** is shown in Fig. 2. As seen, the cleavage of the N1—H9 bond together with the formation of the

Table 1

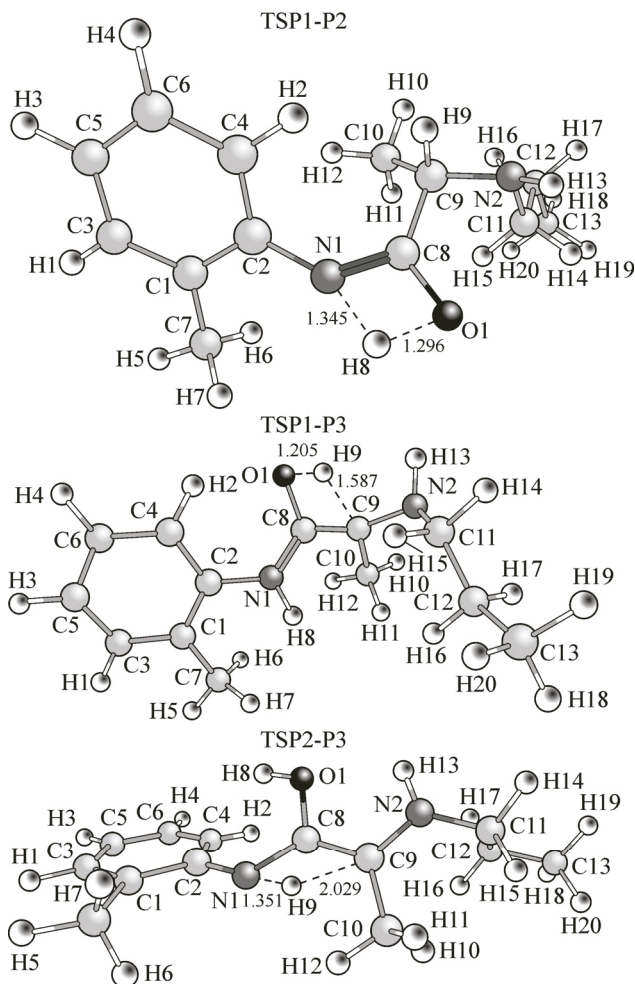
*Selected structural parameters for P1, P2 and P3 tautomers of the prilocaine*

Parameter	P1	P2	P3	TSP1—P2	TSP1—P3	TSP2—P3
Bond length, Å						
N1—H8	1.00	2.43	1.00	1.34	1.01	2.52
O1—H8	3.14	0.96	3.11	1.29	3.18	0.96
C8—O1	1.22	1.36	1.37	1.30	1.30	1.38
C9—H9	1.09	1.09	2.45	1.09	1.58	2.02
C8—N1	1.36	1.27	1.39	1.31	1.33	1.46
O1—H9	2.76	2.57	0.96	3.11	1.20	2.39
C8—C9	1.55	1.52	1.34	1.52	1.46	1.39
N1—H9	2.98	3.12	1.01	2.88	2.90	1.35
Angle, deg.						
C4—C2—N1	122.4	120.4	121.7	121.8	121.3	125.7
C2—N1—H8	114.9	69.7	116.0	151.9	115.5	71.1
C2—N1—C8	129.8	121.2	125.2	133.7	129.9	116.6
H8—N1—C8	115.2	31.2	115.0	73.6	114.3	49.8
N1—C8—O1	123.8	125.5	111.1	105.9	122.7	119.8
N1—C8—C9	116.6	123.7	125.0	131.2	128.4	121.6
O1—C8—C9	119.4	110.6	123.7	122.7	108.5	114.5
C8—C9—H9	103.3	105.0	51.0	105.2	63.1	37.3
C8—C9—N2	111.1	112.7	120.9	114.2	115.0	118.8
C9—N2—C11	116.2	117.1	118.4	118.1	120.0	124.9
Dihedral angle, deg.						
C6—C4—C2—N1	179.3	175.9	-179.4	-178.0	-179.9	-179.5
H8—N1—C8—O1	-177.4	0.1	-141.1	0.0	-177.3	13.1
O1—C8—C9—N2	35.1	55.1	5.7	-1.0	75.8	-3.4
C1—C2—N1—H8	4.3	-111.6	25.6	-53.4	-20.4	-137.9
C9—C8—N1—H8	5.2	179.9	35.3	179.8	8.5	169.7
C2—N1—C8—O1	1.8	3.4	61.5	172.6	8.5	39.6
C2—N1—C8—C9	-175.5	-176.9	-122.1	-7.6	-165.6	-163.8

Table 2

*Relative energies (kJ/mol) of P1—P3 tautomers of the prilocaine*

Species	Gas phase	PCM model	Species	Gas phase	PCM model
<b>P1</b>	0.0	0.0	<b>TS P1-P2</b>	171.29	179.07
<b>P2</b>	45.93	54.60	<b>TS P1-P3</b>	270.47	281.68
<b>P3</b>	74.35	96.65	<b>TS P2-P3</b>	326.75	330.11



In the solution phase, the Gibbs free energy difference between the most stable tautomer (**P1**) and non-stable **P2** and **P3** tautomers are 46.63 and 89.36 kJ/mol. Hence, using Eq. (1), the amount of the **P2** and **P3** tautomers in an aqueous solution of the prilocaine is predicted to be negligible.

**IR and NMR spectra.** Herein, the IR and NMR spectra of the most stable tautomer of the prilocaine (**P1**) were assigned theoretically using valuable DFT methods. The obtained results were compared with the experimental ones.

The vibrational modes of **P1** were analyzed by comparing the DFT and experimental IR spectra of the prilocaine. Assignments of the selected vibrational frequencies are listed in Table 3. Some medium to strong bands in the 3500–2500 cm<sup>-1</sup> spectral range of the prilocaine can be attributed to the overlapping of N—H and C—H stretching vibrations [10–13, 21, 22]. Deconvolution of this region is given in Table 3.

A very strong band at 1706 cm<sup>-1</sup> is related to the stretching modes of the carbonyl moiety. Also, a very strong band appears at 1539 cm<sup>-1</sup>, which can be attributed to the stretching modes of the C8=N1 bond and the in-plane bending mode of N1—H8.

The DFT calculated <sup>1</sup>H NMR chemical shifts ( $\delta$ ) for the **P1** tautomer of the prilocaine are gathered in Table 4, together with the experimental ones for comparison. The atomic positions in the molecule are numbered as in Fig. 1.

Good consistency between the calculated chemical shifts and vibrational frequencies and the corresponding experimental values are observed, confirming the suitability of the optimized geometry for **P1** as the most stable tautomer of the prilocaine. Also, the obtained results show the assignment of the spectra of the prilocaine, which can also be used as a data bank for the identification of similar compounds.

Fig. 2. Optimized geometries for the **TSP1—P2**, **TSP1—P3**, and **TSP2—P3** species

C9—H9 bond is clear. For the **P2** tautomer, the N1—H9 and C9—H9 bond lengths are 3.12 and 1.09 Å, respectively. In **TSP2—P3**, these bond lengths are 1.35 and 2.02 Å, respectively, which are 1.01 and 2.45 Å in the optimized geometry of the **P3** tautomer, respectively.

**P1** can tautomerize to **P2** and **P3** tautomers through two parallel reactions: **P1**↔**P3** and **P2**↔**P3** tautomerizations, respectively. As seen in Table 2, **P2** is more stable than **P3**. Also, the **P1**↔**P2** tautomerization has a lower barrier energy than **P1**↔**P3**. The **P2** tautomer is a kinetically and thermodynamically more favorable product in the tautomerization reaction of the **P1** tautomer.

Considering the equilibrium between the **P1**, **P2**, **P3** tautomers, the value of the tautomeric equilibrium constant ( $K$ ) is calculated by

$$K = \exp\left(-\frac{\Delta G}{RT}\right), \quad (1)$$

where  $\Delta G$ ,  $R$ , and  $T$  are the Gibbs free energy difference between the three tautomers, the gas constant, and the temperature, respectively.

Table 3

*Selected experimental and calculated IR vibrational frequencies ( $\text{cm}^{-1}$ ) of the P1 tautomer*

Experimental*	Calculated**		Vibrational assignment
	Wavenumbers	Intensity, $\text{kJ/mol}$	
444 (w)	434	6	$\delta_{\text{out-of-plane}}$ (benzene ring)
499 (w)	566	20	$\delta_{\text{out-of-plane}}$ (N1—H8)
699 (w)	741	49	$\delta_{\text{out-of-plane}}$ (C—H) aromatic
762 (m)	746	78	$\delta_{\text{out-of-plane}}$ (N2—H13)
938 (w)	972	11	$\nu$ (N2—C11,C12—C13)
999 (w)	1006	7	$\nu$ (C—C) aliphatic
1042 (m)	1030	14	Breathing of the benzene ring + $\delta_{\text{in plane}}$ (C—H)
1112 (m)	1128	130	$\nu_{\text{asym}}$ (C9—N2—C11)
1198 (w)	1221	70	$\nu$ (C2=N1) + $\nu$ (C1—C7)
1254 (m)	1267	51	$\delta_{\text{in plane}}$ (C—H) aromatic
1299 (m)	1285	41	$\nu_{\text{asym}}$ (C=C) benzene ring
1458 (m)	1458	32	$\delta_{\text{wag}}$ (C—H)
1539 (vs)	1501	319	$\nu$ (C8=N1) + $\delta_{\text{in plane}}$ (N1—H8)
1585 (m)	1564	98	$\nu_{\text{sym}}$ (C=C) benzene ring
1706 (vs)	1669	216	$\nu$ (C8=O1)
2439 (m)	2892	16	$\nu$ (C9—H9)
2528 (m)	2855—2913	29—35	$\nu_{\text{sym}}$ (CH <sub>2</sub> ,CH <sub>3</sub> ) aliphatic
2717 (s)	2924—2994	18—95	$\nu_{\text{asym}}$ (CH <sub>2</sub> ,CH <sub>3</sub> ) aliphatic
2979 (s)	3037—3119	6—21	$\nu$ (C—H) aromatic
	3420	9	$\nu$ (N2—H13)
3206 (s)	3510	35	$\nu$ (N1—H8)

\* The experimental results were taken from [ 23 ].

\*\* The calculated vibrational-frequencies were corrected using a scale factor of 0.9614.

Table 4

*Experimental and theoretical <sup>1</sup>H NMR chemical shifts of the prilocaine and its P1 tautomer in a DMSO solution,  $\delta$  (ppm)*

Atomic position	Theor.	Exp.*	Atomic position	Theor.	Exp.*
H13	8.74		H15	2.14	2.52
H2	9.15		H5, H6, H7	2.40	2.17
H1, H4	7.53	7.19—7.30	H10, H11, H12	1.54	1.31
H3	7.28		H16	1.54	1.45
H9	3.59	3.45	H17	1.48	
H8	2.98		H18	1.08	
H14	2.68	2.52	H19, H20	0.72	0.85

\* The experimental results were taken from [ 24 ].

Table 5

*Stabilization energy of hyper conjugative interactions in the NBO basis for the **P1** tautomer of the prilocaine*

Donor NBO	Acceptor NBO	$E(2)$ , kJ/mol	Donor NBO	Acceptor NBO	$E(2)$ , kJ/mol
BD(2) C1—C3	BD*(2) C2—C4	91.96	LP(1) N1	BD*(2) C2—C4	137.69
BD(2) C1—C3	BD*(2) C5—C6	76.45	LP(1) N1	BD*(2) C8—O1	238.97
BD(2) C2—C4	BD*(2) C1—C3	75.11	LP(2) O1	BD*(1) N1—C8	105.04
BD(2) C2—C4	BD*(2) C5—C6	77.04	LP(2) O1	BD*(1) C8—C9	72.02
BD(2) C5—C6	BD*(2) C1—C3	92.67			
BD(2) C5—C6	BD*(2) C2—C4	88.66			

**NBO analysis.** The NBO analysis is a valuable tool to explore the intra- and intermolecular bonding interactions and investigate the charge transfer in chemical compounds. Electron delocalization between the donor NBO( $i$ ) and acceptor NBO( $j$ ) orbitals cause the stabilization of the energy of hyper conjugative interactions ( $E(2)$ ). The amount of  $E(2)$  is a criteria for the degree of interaction between the electron donor and acceptor orbitals. The greater the  $E(2)$ , the greater the electron transfer tendency from the electron donor to the electron acceptor, resulting in higher electron density delocalization, and consequently, leading to a higher stabilization of the system [ 13, 25, 26 ]. The important electron transitions which result in the highest stabilization energy ( $E(2)$ ) for the **P1** tautomer are gathered in Table 5. The  $E(2)$  values were calculated as mentioned in the previously reported works [ 13, 26 ].

As seen, LP(N1)  $\rightarrow$   $\pi^*(\text{C}2—\text{C}4)$  and LP(N1)  $\rightarrow$   $\pi^*(\text{C}8—\text{O}1)$  electron donations lead to the strongest interactions, inducing the highest stabilization energy in the **P1** tautomer. The LP(O1)  $\rightarrow$   $\sigma^*(\text{N}1—\text{C}8)$  and LP(O1)  $\rightarrow$   $\sigma^*(\text{C}8—\text{C}9)$  electron donations together with the  $\pi \rightarrow \pi^*$  transitions of the benzene ring result in the high stabilization energy, too.

The energy gap between the highest occupied molecular orbital (HOMO) and lowest unoccupied molecular orbital (LUMO) frontier orbitals is one of the significant characteristics of molecules, which plays an important role for the electric properties, electronic spectra, and photochemical reactions. The energy gap between the HOMO and LUMO orbitals of the **P1** tautomer of the prilocaine is 4.36 eV. This large energy gap confirms a high stability of the **P1** tautomer [ 13, 27 ].

The 3D distribution map for the HOMO and LUMO orbitals of the **P1** tautomer are shown in Fig. 3. As seen, the HOMO orbital is mainly located on the N2 atom. But the LUMO orbital is localized on the benzene ring and the carbonyl group of the molecule.

## CONCLUSIONS

The prilocaine is an amino amide local anaesthetic drug. In this work, the optimized geometries and energetic characteristics of three possible tautomers of the prilocaine, as well as the kinetics and mechanism of its tautomerization have been theoretically investigated in detail using the DFT methods.

**P1** is the most stable tautomer of the prilocaine, which can be tautomerized to **P2** and **P3** tautomers *via* IPT reactions. In both gas phase and aqueous solution, the **P1**  $\rightleftharpoons$  **P2** tautomerization has a

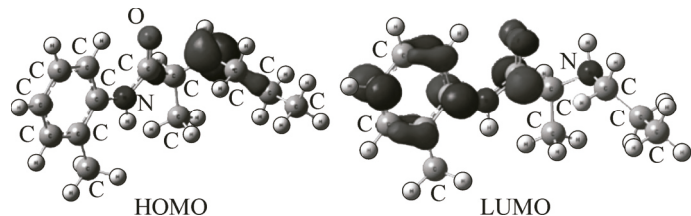


Fig. 3. HOMO and LUMO frontier orbitals of the **P1** tautomer of the prilocaine

lower barrier energy than **P1**↔**P3**. The **P2** tautomer can be tautomerized to **P3**, too, which involves a higher barrier energy than the direct **P1**↔**P3** tautomerization.

The DFT computed chemical shifts and vibrational frequencies are in good agreement with the experimental ones, confirming the validity of the optimized geometry for **P1** as the most stable tautomer of the prilocaine.

The HOMO frontier orbital of the **P1** tautomer is mostly located on the N2 atom, while LUMO is localized on the carbonyl group and the benzene ring. A large HOMO—LUMO energy gap confirms a high stability of this tautomer.

#### REFERENCES

1. Scott D.B., Jebson P.J.R. // Br. J. Anaesth. – 1972. – **44**. – P. 1040 – 1049.
2. Jastak J.T., Yagiela J.A., Donaldson D. Local Anesthesia of the Oral Cavity. – Philadelfia, PA: WB Saunders, 1995. – P. 297 – 298.
3. Polley L.S., Columb M.O., Naughton N.N., Wagner D.S., van de Ven C.J. // Anesthesiology. – 1999. – **90**. – P. 944 – 950.
4. Cereda C.M.S., Brunetto G.B., de Araújo D R., de Paula E. // Can. J. Anaesth. – 2006. – **53**. – P. 1092 – 1097.
5. Cereda C.M.S., de Araujo D.R., Brunetto G.B., De Paula E. // J. Pharm. Pharm. Sci. – 2004. – **7**. – P. 235 – 240.
6. Bartholomew K., Sloan J.P. // Arch. Emerg. Med. – 1990. – **7**. – P. 189 – 195.
7. Hjelm M., Holmdahl M.H. // Acta Anaesthesiol. Scand. – 1965. – **9**. – P. 161 – 170.
8. Covino B.G. // Br. J. Anaesth. – 1986. – **58**. – P. 701 – 716.
9. Löfgren N., Tegnér C. // Acta Chem. Scand. – 1960. – **14**. – P. 486 – 490.
10. Liu Y., Hou J.B., Liu X.X., Miao F.M., Zhao Y.F. // J. Struct. Chem. – 2009. – **50**. – P. 835 – 840.
11. Beyramabadi S.A., Morsali A., Javan-Khoshkholgh M., Esmaeili A.A. // J. Struct. Chem. – 2012. – **53**. – P. 460 – 467.
12. Beyramabadi S.A., Morsali A., Vahidi S.H., Javan-Khoshkholgh M., Esmaeili A.A. // J. Struct. Chem. – 2012. – **53**. – P. 665 – 675.
13. Sadeghzade Z., Beyramabadi S.A., Morsali A. // Spectrochim. Acta, Part A. – 2015. – **138**. – P. 637 – 642.
14. Vakili M., Dolati F., Tayyari S.F., Rajabi O., Salari R. 15th Iranian Chemistry Congress, 2011.
15. Frisch M.J. et al. Gaussian 03, Revision B.03. – Pittsburgh, PA: Gaussian Inc., 2003.
16. Lee C., Yang W., Parr R.G. // Phys. Rev. B. – 1988. – **37**. – P. 785 – 789.
17. Cammi R., Tomasi J. // J. Comput. Chem. – 1995. – **16**. – P. 1449 – 1458.
18. Young D.C. Computational Chemistry: A Practical Guide for Applying Techniques to Real-World Problems. – John Wiley & Sons, Inc., 2001.
19. Ditchfield R. // Mol. Phys. – 1974. – **27**. – P. 789 – 807.
20. Zhurko G.A., Zhurko D.A. Chemcraft 1.7. <http://www.chemcraftprog.com>.
21. Sanmartín J., García-Deibe A.M., Fondo M., Navarro D., Bermejo M.R. // Polyhedron. – 2004. – **23**. – P. 963 – 967.
22. Ware D.C., Mackie D.S., Brothers P.J., Denny W.A. // Polyhedron. – 1995. – **14**. – P. 1641 – 1646.
23. Rajendiran N., Mohandoss T., Saravanan J. // Spectrochim. Acta, Part A. – 2014. – **132**. – P. 387 – 396.
24. Cabeca L.F., Pickholz M., Paula E., Marsaioli A.J. // J. Phys. Chem. B. – 2009. – **113**. – P. 2365 – 2370.
25. Snehalatha M., Ravikumar C., Hubert Joe I., Sekar N., Jayakumar V.S. // Spectrochim. Acta, Part A. – 2009. – **72**. – P. 654 – 662.
26. Schwenke D.W., Truhlar D.G. // J. Chem. Phys. – 1985. – **82**. – P. 2418 – 2427.
27. Tezer N., Karakus N. // J. Mol. Model. – 2009. – **15**. – P. 223 – 232.